2019

A locally-implicit Lax-Wendroff discontinuous Galerkin scheme with limiters that guarantees moment-realizability for quadrature-based moment closures

Christine Wiersma
Iowa State University

A locally-implicit Lax-Wendroff discontinuous Galerkin scheme with limiters that guarantees moment-realizability for quadrature-based moment closures

by

Christine Wiersma

A thesis submitted to the graduate faculty

in partial fulfillment of the requirements for the degree of

MASTER OF SCIENCE

Major: Applied Mathematics

Program of Study Committee:
James Rossmanith, Major Professor
Jue Yan
Alberto Passalacqua
Rodney Fox

The student author, whose presentation of the scholarship herein was approved by the program of study committee, is solely responsible for the content of this thesis. The Graduate College will ensure this thesis is globally accessible and will not permit alterations after a degree is conferred.

Iowa State University

Ames, Iowa

2019

TABLE OF CONTENTS

ABSTRACT

A polydisperse multiphase flow is one in which one of the thermodynamic phases can be considered discrete while the other is assumed to be continuous. Examples include sprays and bubbly flows. Such flows can be modeled by kinetic models that describe the evolution of a probability density function (PDF) in phase space. Moments of this PDF describe physical observable quantities such as the mass, momentum, and energy in the flow. From a computational perspective, kinetic models are expensive to solve since they require the resolution of a very high-dimensional phase space. In many polydisperse multiphase flow applications, the phase space would consist of the spatial variables (three dimensions), the velocity variables (three dimensions), a size dimension (one dimension), and time (one dimension).

An alternative to kinetic models are so-called fluid models, which instead of evolving the full kinetic distribution function, evolve only a small subset of moments of the PDF. Fluid models are defined on a lower dimensional space than the original distribution function, and as such, are computationally much more tractable. The difficulty with fluid models is that the precise form of the fluid approximation depends on the choice of the moment-closure. In general, finding a suitable robust moment-closure is still an open scientific problem.

In this work, we consider an approach for developing fluid approximations to kinetic equations known as quadrature-based moment-closures. The true distribution function is replaced by a finite set of Dirac delta functions with variable weights and abscissas. After developing this model, we then propose a high-order numerical method using the discontinuous Galerkin (DG) finite element method to discretize the resulting system. In particular, we develop a Lax-Wendroff discontinuous Galerkin method, which allows us to efficiently achieve high-order through a locally-implicit prediction step, followed by a

fully explicit correction step. The key difficulty in applying high-order schemes to nonlinear hyperbolic systems is that the formation of shocks, rarefactions, and vacuum states cause the numerical solution to produce large unphysical oscillations that lead to simulation failures. To remedy these problems, we develop a series of post-processing steps, referred to as limiters, that provably guarantee that the solution remains physical and that suppress unphysical solutions. The resulting method is verified on several shock tube problems.

CHAPTER 1. INTRODUCTION

1.1 Motivation

A multiphase flow is a flow with two or more thermodynamic phases [1, 13]. Examples of multiphase flows include gas bubbles in a liquid, sprays, and free-surface flows (see Figure 1.1). A multiphase flow is considered disperse if one of the thermodynamic phases can be considered discrete while the other is assumed to be continuous. In the example of a bubbly flow, we treat the bubbles as discrete entities and the liquid is assumed to be continuous, while in a spray, the droplets or particles are discrete and the gas or air is continuous. In contrast, a free-surface flow is considered to be multiphase, but it is not disperse since both phases are considered to be continuous. An example of this would be the surface of a body of water and the air that meets it. A polydisperse multiphase flow is a disperse multiphase flow where the particles have varying volumes, masses, etc.. This can be readily seen in a bubbly flow. There are very small bubbles moving quickly through the liquid phase, but there are also large bubbles that have more drag forces acting on them as they move in the continuous phase. The goal of the current work is to develop robust models of polydisperse multiphase flows that are computationally tractable, as well as to develop numerical schemes to solve the equations that arise from these models.

1.2 The Full Kinetic Equation

There are multiple equations that describe the evolution of a multiphase flow. Some notable examples include the Fokker-Planck or Kolmogorov forward equation (1931), the Vlasov equation (1938), and the Boltzmann equation (1872). We will focus our work on the kinetic Boltzmann equation, which describes the statistical behavior of a system not in thermodynamic equilibrium.

(a) (b) (c)

Figure 1.1: Examples of a multiphase flow. The panels show (a) a bubbly flow (https://www.stocksy.com/1423737/air-bubbles-in-water), which is considered a disperse multiphase flow, (b) a spray (iStockphoto), which is also considered a disperse multiphase flow, and (c) a free-surface flow (PaulPaladin), which is a multiphase flow, but is not disperse.

The standard class of models for polydisperse multiphase flow are so-called population balance equations of the following form:

$$\frac{\partial f}{\partial t} + \underline{v} \cdot \frac{\partial f}{\partial \underline{x}} + \underline{\mathcal{F}} \cdot \frac{\partial f}{\partial \underline{v}} + \frac{\partial}{\partial \xi}[G(\xi) f] = \mathbb{C}(f), \tag{1.1}$$

where f is the distribution function, $\underline{v}$ is the velocity coordinate, which is independent of x and t, x is the spatial variable, and t is the time variable. Additionally, $\underline{\mathcal{F}}$ is the forcing term which includes lift, drag, gravity, and other forces acting on the particles. In the third term, ξ is the size variable and G is the term that describes the changes in size of the particles, which can include particles splitting into two smaller particles or two particles joining to become one larger particle. Finally, there is a collision term $\mathbb{C}$ which describes the interactions particles have with each other. In equation (1.1) f is the probability distribution function, giving the probability of finding a particle at time t, with position $\underline{x}$, and velocity $\underline{v}$. Using a statistical approach and investigating the probability distribution function allows us to examine the flow without tracking individual particles, which is computationally expensive.

The ultimate goal of the current research is consider the full 3D3V equation as described by (1.1), but for the remainder of the current work, we will take a step backwards and simplify the problem significantly. We will spend the remainder of this thesis working in one dimension with the 1D1V kinetic Boltzmann equation as described in the next section.

1.3 A Simplified Setting

The 1D1V kinetic Boltzmann equation or the 1D1V Vlasov equation is given by

$$f_{,t} + v\, f_{,x} = \mathbb{C}(f), \tag{1.2}$$

where $f = f(t, x, v)$ is the same probability distribution function. We can define the mass density and other moments by integrating $v^k f$ with respect to v:

$$\int_{-\infty}^{\infty} v^\ell\, f\, dv = \begin{cases} \rho & \ell = 0, \\ \rho u & \ell = 1, \\ \rho u^2 + p & \ell = 2, \\ \rho u^3 + +3pu + q & \ell = 3, \\ \rho u^4 + 6pu^2 + 4qu + \frac{p^2}{\rho} + \frac{q^2}{p} + k & \ell = 4. \end{cases} \tag{1.3}$$

This hierarchy gives the evolution equation for each moment:

$$\left(\int_{-\infty}^{\infty} v^\ell\, f\, dv\right)_{,t} + \left(\int_{-\infty}^{\infty} v^{\ell+1}\, f\, dv\right)_{,x} = \int_{-\infty}^{\infty} v^\ell\, \mathbb{C}(f)\, dv, \tag{1.4}$$

for $\ell = 0, 1, 2, \ldots$. If we consider all the moments (of which there are an infinite number), then the moment equations are completely equivalent to the original 1D1V kinetic equation (1.2). However, if we truncate this moment hierarchy to some small number of moments, we have what referred to a fluid approximation.

Therefore, an alternative to solving kinetic models such as (1.2), are fluid models, which instead of evolving the full kinetic distribution function, evolve only a small subset of moments of the PDF. Fluid models are defined on a lower dimensional space than the original distribution function, and as such, are computationally much more tractable. The difficulty with fluid models is that the precise form of the fluid approximation depends on the choice of the moment-closure. In general, finding a suitable robust moment-closure is still an open scientific problem.

1.4 Scope of This Work

The kinetic Boltzmann equation is an equation that can be used to describe disperse multiphase flows that are not in equilibrium. We can approximate the kinetic description via a fluid model, but we must close the system. In this work we study a particular strategy for closing the moment hierarchy: the hyperbolic quadrature based moment closure [18]. The true distribution function is replaced by a finite set of Dirac delta functions with variable weights and abscissas. After closing the system, we are left with the following fluid system:

$$\begin{bmatrix} \rho \\ u \\ p \\ q \\ k \end{bmatrix}_{,t} + \begin{bmatrix} u & \rho & 0 & 0 & 0 \\ 0 & u & \frac{1}{\rho} & 0 & 0 \\ 0 & 3p & u & 1 & 0 \\ -\frac{p^2}{\rho^2} & 4q & -\frac{q^2}{p^2} - \frac{p}{\rho} & u + \frac{2q}{p} & 1 \\ 0 & 5k & -\frac{2kq}{p^2} & \frac{2k}{p} & u \end{bmatrix} \begin{bmatrix} \rho \\ u \\ p \\ q \\ k \end{bmatrix}_{,x} = 0, \tag{1.5}$$

where ρ is the density, u is the macroscopic fluid velocity, p is the thermal pressure, and k is the kurtosis.

We investigate the effects of this choice of closure on the Boltzmann equation, how the results align with moment-realizability conditions obtained from the Hamburger moment problem, and the preservation of the hyperbolicity of the resulting system of equations.

After developing this model, we then propose a high-order numerical method using the discontinuous Galerkin (DG) finite element method to discretize the resulting system. In particular, we develop a Lax-Wendroff discontinuous Galerkin method, which allows us to efficiently achieve high-order through a locally-implicit prediction step, followed by a fully explicit correction step. The key difficulty in applying high-order schemes to nonlinear hyperbolic systems is that the formation of shocks, rarefactions, and vacuum states cause the numerical solution to produce large unphysical oscillations that lead to simulation failures. To remedy these problems, we develop a series of post-processing steps, referred to as limiters, that provably guarantee that the solution remains physical and that suppress unphysical solutions. The resulting method is verified on several shock tube problems.

A brief outline of this thesis is discussed next. In Chapter 2 we define the necessary terminology to discuss the moment closure problem, introduce the Hamburger moment problem, and develop the hyperbolic quadrature based moment closure. Chapter 3 describes the locally-implicit Lax-Wendroff discontinuous Galerkin method. We examine the method closely and discuss its merits as a high order method. Chapter 4 next discusses the limiters that were implemented to enforce the hyperbolicity conditions and to damp unphysical oscillations. This method and the limiters were implemented on three problems in Python and the results are shown in Chapter 5. Final conclusions and a discussion on future work are discussed in Chapter 6. All examples are written in a freely-available open-source Python code [4].

CHAPTER 2. MOMENT CLOSURE

The 1D1V Boltzmann equation, which describes the dynamics of a gas, has the following form:

$$f_{,t} + v f_{,x} = C(f), \tag{2.1}$$

where $f(t,x,v) : \mathbb{R}^+ \times \mathbb{R} \times \mathbb{R} \mapsto \mathbb{R}$ is the probability density function (PDF) that characterizes the state of the gas, (t,x,v) are the time, space, and velocity variables, respectively, and $C(f)$ is the collision operator.

The distribution function, f, is itself not physically observable; however, its moments represent various physically observable quantities, e.g.,

$$\rho(t,x) := \int_{-\infty}^{\infty} f(t,x,v)\, dv, \qquad \text{(mass density)}, \tag{2.2}$$

$$\rho u(t,x) := \int_{-\infty}^{\infty} v\, f(t,x,v)\, dv, \qquad \text{(momentum density)}, \tag{2.3}$$

$$\mathcal{E}(t,x) := \int_{-\infty}^{\infty} v^2\, f\, dv, \qquad \text{(kinetic energy density)}. \tag{2.4}$$

One can also define the *primitive* form of the moments, e.g.,

$$\rho(t,x) := \int_{-\infty}^{\infty} f(t,x,v)\, dv, \qquad \text{(mass density)}, \tag{2.5}$$

$$u(t,x) := \frac{1}{\rho} \int_{-\infty}^{\infty} v f(t,x,v)\, dv, \qquad \text{(macroscopic velocity)}, \tag{2.6}$$

$$p(t,x) := \int_{-\infty}^{\infty} (v-u)^2\, f\, dv, \qquad \text{(pressure)}, \tag{2.7}$$

$$q(t,x) := \int_{-\infty}^{\infty} (v-u)^3\, f\, dv, \qquad \text{(heat flux)}, \tag{2.8}$$

$$k(t,x) := \int_{-\infty}^{\infty} (v-u)^4\, f\, dv - \left(\frac{p^3 + \rho q^2}{\rho p} \right), \qquad \text{(kurtosis)}. \tag{2.9}$$

Taking moments directly of the 1D1V Boltzmann equation (2.1) results in so-called *fluid*

equations, all of which are of the form:

$$\left(\int_{-\infty}^{\infty} v^{\ell}\, f\, dv\right)_{,t} + \left(\int_{-\infty}^{\infty} v^{\ell+1}\, f\, dv\right)_{,x} = \int_{-\infty}^{\infty} v^{\ell}\, C\, dv \quad \Longrightarrow \quad \mathbb{M}_{\ell,t} + \mathbb{M}_{\ell+1,x} = \mathbb{C}_{\ell}, \tag{2.10}$$

where $\ell = 0, 1, 2, \ldots,$

$$\mathbb{M}_{\ell} := \int_{-\infty}^{\infty} v^{\ell}\, f(t,x,v)\, dv, \quad \text{and} \quad \mathbb{C}_{\ell} := \int_{-\infty}^{\infty} v^{\ell}\, \mathcal{C}(f)\, dv. \tag{2.11}$$

The 1D1V Boltzmann equation (2.1) is a scalar partial differential equation (PDE) in a two-dimensional phase space plus time, while the fluid equations (2.10) are a system of PDEs in one-space dimension plus time. In practice, it may be possible to obtain a reasonably accurate solution of the Boltzmann equation (2.1) by instead solving a finite subset of the fluid equations. However, there is a clear problem with the fluid equations: if we choose to evolve a finite subset of fluid equations, say for $\ell = 0, 1, 2, \ldots, S$, then the final equation in the moment hierarchy:

$$\mathbb{M}_{S,t} + \mathbb{M}_{S+1,x} = \mathbb{C}_{S}, \tag{2.12}$$

requires knowledge of the next moment, $\mathbb{M}_{S+1}$, which we are not explicitly evolving. This conundrum is known as the *moment-closure problem*, which we formulate more precisely below.

Definition 2.0.1 (*The moment-closure problem)***.** Given a finite number of moments:

$$\{\mathbb{M}_{\ell} : \ \ell = 0, 1, 2, \ldots, S\}, \tag{2.13}$$

find a function $f^{\star}(v) \geq 0$ such that

$$\int_{-\infty}^{\infty} v^{\ell}\, f^{\star}(v)\, dv = \mathbb{M}_{\ell} \quad \text{for} \quad \ell = 0, 1, 2, \ldots, S. \tag{2.14}$$

Once the function $f^{\star}(v)$ has been constructed, we approximate the missing moment in (2.12) as follows:

$$\mathbb{M}_{S+1} \approx \mathbb{M}^{\star}_{S+1} := \int_{-\infty}^{\infty} v^{S+1}\, f^{\star}(v)\, dv. \tag{2.15}$$

□

If the moment-closure problem is solvable by some PDF, then we say the moments are **realizable**.

Definition 2.0.2 (*Moment-realizability)*. The finite set of moments:

$$\{\mathbb{M}_\ell : \ell = 0, 1, 2, \ldots, S\}, \tag{2.16}$$

are **realizable** if there exists a probability density $f^\star(v) \geq 0$ such that

$$\int_{-\infty}^{\infty} v^\ell \, f^\star(v) \, dv = \mathbb{M}_\ell \quad \text{for} \quad \ell = 0, 1, 2, \ldots, S. \tag{2.17}$$

□

In order to solve the moment-closure problem in practice, we will not search for some arbitrary distribution function, $f^\star(v)$; instead we will look for a function from a predetermined family of distribution functions that are parameterized by $S + 1$ free parameters. If we are able to find a particular distribution function from this family, we see that the moments are **invertible** with respect to the parameterized family.

Definition 2.0.3 (*Moment-invertibility)*. Let $f^\star(v; \alpha_0, \alpha_1, \alpha_2, \ldots, \alpha_S)$ be a family of probability density functions parameterized by $\alpha_0, \alpha_1, \alpha_2, \ldots, \alpha_S$. We say that the moment-closure problem is **invertible** if there exists a set of parameters:

$$\{\alpha_\ell^\star : \ell = 0, 1, 2, \ldots, S\}, \tag{2.18}$$

such that

$$\int_{-\infty}^{\infty} v^\ell \, f^\star(v; \alpha_0^\star, \alpha_1^\star, \alpha_2^\star, \ldots, \alpha_S^\star) \, dv = \mathbb{M}_\ell \quad \text{for} \quad \ell = 0, 1, 2, \ldots, S. \tag{2.19}$$

□

Note that moment-realizability is necessary for moment-invertibility. However, moment-realizability is not sufficient for moment-invertibility, since it is possible to choose a particular family of distribution functions that realizes a smaller portion of moment space than the full class of positive distribution functions.

2.1 Hamburger Moment Problem

In this section we briefly review the problem of moment-realizability. As stated above in Definition 2.0.1, we are looking for the existence of some PDF $f^\star \geq 0$ that realizes moments $\mathbb{M}_0, \ldots, \mathbb{M}_S$:

$$\mathbb{M}_\ell = \int_{-\infty}^{\infty} v^\ell f^\star(v)\, dv \quad \text{for} \quad \ell = \mathbb{M}_0, \ldots, \mathbb{M}_S. \tag{2.20}$$

It is useful to introduce rescaled moments in the following rescaled velocity coordinate:

$$s = \frac{v-u}{\sqrt{T}}, \tag{2.21}$$

such that

$$\widetilde{\mathbb{M}}_\ell := \frac{\sqrt{T}}{\rho} \int_{-\infty}^{\infty} s^\ell f(\sqrt{T}s + u)\, ds, \tag{2.22}$$

where u is the aforementioned macroscopic velocity and $T = p/\rho$ is the temperature. We note that this mapping only exists if

$$\rho > 0 \quad \text{and} \quad p > 0, \tag{2.23}$$

and hence $T > 0$. The first three rescaled moments are then simply:

$$\widetilde{\mathbb{M}}_0 = 1,\ \widetilde{\mathbb{M}}_1 = 0,\ \widetilde{\mathbb{M}}_2 = 1.$$

The Hamburger Moment Problem poses the following question: given a finite number of these rescaled moments, does there exist a positive distribution function that realizes the given moments? The solution is that there does exist a positive distribution function if and only if the Hankel matrix is positive definite, where the Hankel matrix is given by

$$\mathcal{H} = \begin{bmatrix} 1 & 0 & 1 & \iddots \\ 0 & 1 & \widetilde{\mathbb{M}}_3 & \iddots \\ 1 & \widetilde{\mathbb{M}}_3 & \widetilde{\mathbb{M}}_4 & \iddots \\ \iddots & \iddots & \iddots & \iddots \end{bmatrix}. \tag{2.24}$$

For example, in the five-moment case, $S = 4$, which is the relevant case in the current work, we see that this is satisfied when

$$\widetilde{\mathbb{M}}_4 \geq 1 + \widetilde{\mathbb{M}}_3^2, \tag{2.25}$$

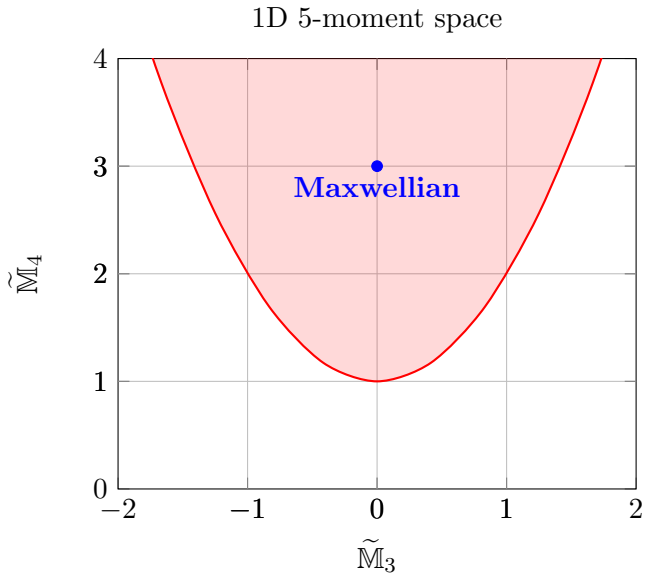

Figure 2.1: Region in moment-space for the 5-moment case (i.e., $S = 4$) where it is possible to find a positive distribution function that realizes the given moments. The blue dot is the location in moment-space of thermodynamic equilibrium (i.e., the Maxwellian distribution).

which we depict in Figure 2.1. Written in terms of primitive variables and combined with condition (2.23), the moment-realizability condition for $S = 4$ (i.e., the five-moment case) is

$$\rho > 0, \quad p > 0, \quad k > 0. \tag{2.26}$$

2.2 Classical moment closures

There are many different moment closure methods that have been proposed, and these different methods have benefits and challenges. In the subsections below, we briefly mention two of the most popular moment-closures.

2.2.1 Grad's moment closure

One of the first methods proposed was Grad's moment closure [7]. This closure approximates the probability distribution function by

$$f^\star(s) = \frac{e^{-\frac{s^2}{2}}}{\sqrt{2\pi T}} \left[\rho + \sum_{k=3}^{N} T^{-\frac{k}{2}} \alpha_k \psi_k(s) \right], \tag{2.27}$$

where $\psi_k(s)$ are Hermite polynomials, and $\underline{\alpha}$ are the Hermite coefficients that serve as this method's free parameters. Grad's closure is problematic because it produces an approximate function, $f^\star$, that is not a proper probability density function, since it is comprised of a Maxwellian (which is positive) multiplied by a high-order Hermite polynomial (which in general is not positive). Additionally, the closure is not guaranteed to be hyperbolic in the range over which the Hamburger moment problem is realizable.

2.2.2 Maximum entropy closure

Another closure that has been studied is the maximum entropy closure, see Dreyer [3], Müller and Ruggeri [15], and Levermore [12]. This closure approximates the distribution function by an exponential:

$$f^\star(v) = e^{\underline{\alpha} \cdot \underline{\Phi}(v)}, \tag{2.28}$$

with parameters $\underline{\alpha}$. With this closure we are guaranteed positivity of $f^\star$ because it is an exponential. Furthermore, it has been shown that this closure results in a symmetric hyperbolic moment system.

However, this closure also has its share of difficulties. First it is non-trivial to invert the equation to find $\underline{\alpha}$. Even more problematic, in an important paper appearing in 2000, Junk [9] found that with this closure there is an area in the region of moment-realizability, where the numerical fluxes become singular, so even though we have a positive distribution function, the equations break down in other ways. Worst of all, these singular fluxes include the point in moment space that represents thermodynamic equilibrium.

2.3 Hyperbolic Quadrature Based Moment Closure

In this work we chose to utilize a different closure than those we have discussed above. This closure was developed by Fox et al. [18], and is examined in detail in this section.

Recall the moment closure problem

$$\left(\int_{-\infty}^{\infty} v^{\ell}\, f\, dv\right)_{,t} + \left(\int_{-\infty}^{\infty} v^{\ell+1}\, f\, dv\right)_{,x} = \int_{-\infty}^{\infty} v^{\ell}\, C(f)\, dv, \tag{2.29}$$

for $\ell = 1, 2, \ldots$ (1.4). Fox et al. [5] conceived the idea to use three delta functions that are defined on certain Gauss-Radau quadrature points approximate f:

$$f \approx f^{\star} = \omega_1 \delta(v - \mu_1) + \omega_2 \delta(v - u) + \omega_3 \delta(v - \mu_3), \tag{2.30}$$

where two of the delta distributions are at unknown locations μ_1, μ_3 and the last delta distribution is fixed at the velocity, u. Each of the distributions is weighted by $\omega_1, \omega_2, \omega_3$. This results in the following moment-inversion problem:

$$\begin{aligned}
\int_{-\infty}^{\infty} f^{\star}(v)\, dv = \int_{-\infty}^{\infty} f(v)\, dv \quad &\Longrightarrow \quad \omega_1 + \omega_2 + \omega_3 = \rho, \\
\int_{-\infty}^{\infty} v f^{\star}(v)\, dv = \int_{-\infty}^{\infty} v f(v)\, dv \quad &\Longrightarrow \quad \omega_1\mu_1 + \omega_2 u + \omega_3\mu_3 = \rho u, \\
\int_{-\infty}^{\infty} v^2 f^{\star}(v)\, dv = \int_{-\infty}^{\infty} v^2 f(v)\, dv \quad &\Longrightarrow \quad \omega_1\mu_1^2 + \omega_2 u^2 + \omega_3\mu_3^2 = \rho u^2 + p, \\
\int_{-\infty}^{\infty} v^3 f^{\star}(v)\, dv = \int_{-\infty}^{\infty} v^3 f(v)\, dv \quad &\Longrightarrow \quad \omega_1\mu_1^3 + \omega_2 u^3 + \omega_3\mu_3^3 = \rho u^3 + 3pu + q, \\
\int_{-\infty}^{\infty} v^4 f^{\star}(v)\, dv = \int_{-\infty}^{\infty} v^4 f(v)\, dv \quad &\Longrightarrow \quad \omega_1\mu_1^4 + \omega_2 u^4 + \omega_3\mu_3^4 = \\
&\qquad\qquad \rho u^4 + 6pu^2 + 4qu + \frac{p^2}{\rho} + \frac{q^2}{p} + k.
\end{aligned} \tag{2.31}$$

We want to find ω_1, ω_2, ω_3, μ_1, and μ_2 such that this system is satisfied. To do this, we pretend temporarily that ω_2 is known and move it over to the right hand side of each equation in the system (2.31). We also momentarily ignore the fifth equation. This results

in the following four equations:

$$\begin{aligned}
\omega_1 + \omega_3 &= (\rho - \omega_2)\,, \\
\omega_1\mu_1 + \omega_3\mu_3 &= (\rho - \omega_2)\,u, \\
\omega_1\mu_1^2 + \omega_3\mu_3^2 &= (\rho - \omega_2)\,u^2 + p, \\
\omega_1\mu_1^3 + \omega_3\mu_3^3 &= (\rho - \omega_2)\,u^3 + 3pu + q.
\end{aligned} \tag{2.32}$$

Solving this system is equivalent to finding the quadrature points and weights of a Gaussian quadrature formula. In particular, we need to devise the two-point Gaussian quadrature formula for the following integral:

$$\int_{-\infty}^{\infty} g(v)\hat{f}(v)\,dv \approx \omega_1 g(\mu_1) + \omega_3 g(\mu_3), \tag{2.33}$$

where

$$\int_{-\infty}^{\infty} v^k \hat{f}(v)\,dv = \begin{cases} \rho - \omega_2, & \text{if} \quad k = 0, \\ (\rho - \omega_2)u, & \text{if} \quad k = 1, \\ (\rho - \omega_2)u^2 + p, & \text{if} \quad k = 2, \\ (\rho - \omega_2)u^3 + 3pu + q, & \text{if} \quad k = 3. \end{cases} \tag{2.34}$$

The goal is to make this quadrature exact for $g(v) = 1$, v, v^2, v^3, which will give us the solution to (2.32). This is accomplished by finding polynomials that are orthogonal in the $\hat{f}(v)$ weighted $L^2[-\infty, \infty]$ norm. We begin with a polynomial of degree 0, $P_0(v) = 1$, and a polynomial of degree 1, $P_1(v) = v + b$. We then enforce the orthogonality condition:

$$\begin{aligned}
\int_{-\infty}^{\infty} P_0(v)P_1(v)\hat{f}(v)\,dv &= \int_{-\infty}^{\infty} (v + b)\hat{f}(v)\,dv = 0 \\
&= \int_{-\infty}^{\infty} v\hat{f}(v)\,dv + b\int_{-\infty}^{\infty} \hat{f}(v)\,dv = 0 \\
&= (\rho - \omega_2)u + b(\rho - \omega_2) = 0,
\end{aligned} \tag{2.35}$$

by (2.34). Therefore, we see that $b = -u$ and $P_1(v) = v - u$. Next, we let $P_2(v) =$

$v^2 + c(v-u) + d$, and we force orthogonality of $P_2(v)$ with $P_0(v)$ and $P_1(v)$. First,

$$\begin{aligned}\int_{-\infty}^{\infty} P_0(v)P_2(v)\hat{f}(v)\,dv &= \int_{-\infty}^{\infty} (v^2 + c(v-u) + d)\hat{f}(v)\,dv = 0 \\ &= \int_{-\infty}^{\infty} v^2\hat{f}(v)\,dv + \int_{-\infty}^{\infty} c(v-u)\hat{f}(v)\,dv + \int_{-\infty}^{\infty} d\hat{f}(v)\,dv = 0 \\ &= (\rho-\omega_2)u^2 + p + 0 + (\rho-\omega_2)d = 0,\end{aligned} \tag{2.36}$$

which gives $d = u^2 - \frac{p}{\rho}$. Second,

$$\begin{aligned}\int_{-\infty}^{\infty} P_1(v)P_2(v)\hat{f}(v)\,dv &= \int_{-\infty}^{\infty} (v-u)(v^2 + c(v-u) + d)\hat{f}(v)\,dv = 0 \\ &= \int_{-\infty}^{\infty} (v-u)v^2\hat{f}(v)\,dv + \int_{-\infty}^{\infty} c(v-u)^2\hat{f}(v)\,dv \\ &\qquad + \int_{-\infty}^{\infty} (v-u)d\hat{f}(v)\,dv = 0 \\ &= \int_{-\infty}^{\infty} v^3\hat{f}(v)\,dv - u\int_{-\infty}^{\infty} v^2\hat{f}(v)\,dv + c\int_{-\infty}^{\infty} (v-u)^2\hat{f}(v)\,dv \\ &= (\rho-\omega_2)u^3 + 3pu + q - u((\rho-\omega_2) + p) + cp = 0.\end{aligned} \tag{2.37}$$

Thus, we find that $c = \frac{2pu+q}{-p}$, and we can plug c and d into $P_2(v)$ to obtain

$$P_2(v) = v^2 + u^2 - 2uv - \frac{p}{\rho-\omega_2} + \frac{qu-qv}{p}. \tag{2.38}$$

The polynomial $P_2(v)$ has the following roots, which are also the locations of the quadrature points:

$$\mu_1 = \frac{q}{2p} + u + \frac{\sqrt{4p^3 + q^2\rho - q^2\omega_2}}{2p\sqrt{\rho-\omega_2}}, \qquad \mu_3 = \frac{q}{2p} + u - \frac{\sqrt{4p^3 + q^2\rho - q^2\omega_2}}{2p\sqrt{\rho-\omega_2}}. \tag{2.39}$$

Substituting this result into the first two equations of (2.32), allows us to also obtain the quadrature weights:

$$\omega_1 = \frac{\rho}{2} - \frac{\omega_2}{2} - \frac{pq - \omega_2 q}{2\sqrt{\frac{q^2\rho + q^2\omega_2 + 4p^3}{\rho-\omega_2}}}, \qquad \omega_3 = \frac{\rho}{2} - \frac{\omega_2}{2} + \frac{pq - \omega_2 q}{2\sqrt{\frac{q^2\rho + q^2\omega_2 + 4p^3}{\rho-\omega_2}}}. \tag{2.40}$$

Once we have found μ_1, μ_2, ω_1, and ω_3 in terms of ω_2, we can definitively determine ω_2 by enforcing the neglected fifth equation in (2.31):

$$\omega_2 = \rho - \frac{p^3}{p(k + \frac{p^2}{\rho} + \frac{q^2}{p}) - q^2}. \tag{2.41}$$

Putting all of these results together yields:

$$\begin{aligned} M_5 \approx M_5^\star := \int_{-\infty}^{\infty} v^5 f^\star(v)\, dv &= \omega_1\mu_1^5 + \omega_2 u^5 + \omega_3\mu_3^5 \\ &= \rho u^5 + 10pu^3 + 10qu^2 + 5\left(k + \frac{p^2}{\rho} + \frac{q^2}{p}\right)u \\ &\quad + \frac{2q\left(k + \frac{p^2}{\rho} + \frac{q^2}{p}\right)}{p} - \frac{q^3}{p^2}. \end{aligned} \tag{2.42}$$

Hence, written as a conservation law of the form

$$\underline{q}_{,t} + \underline{f}(\underline{q})_{,x} = \underline{0}, \tag{2.43}$$

we obtain the following equation (all collisions have been neglected in this expression):

$$\begin{bmatrix} \rho \\ \rho u \\ \rho u^2 + p \\ \rho u^3 + +3pu + q \\ \rho u^4 + 6pu^2 + 4qu + \frac{p^2}{\rho} + \frac{q^2}{p} + k \end{bmatrix}_{,t} + \begin{bmatrix} \rho u \\ \rho u^2 + p \\ \rho u^3 + +3pu + q \\ \rho u^4 + 6pu^2 + 4qu + \frac{p^2}{\rho} + \frac{q^2}{p} + k \\ M_5^\star \end{bmatrix}_{,x} = 0. \tag{2.44}$$

In terms of primitive variables, the system becomes

$$\begin{bmatrix} \rho \\ u \\ p \\ q \\ k \end{bmatrix}_{,t} + \begin{bmatrix} u & \rho & 0 & 0 & 0 \\ 0 & u & \frac{1}{\rho} & 0 & 0 \\ 0 & 3p & u & 1 & 0 \\ -\frac{p^2}{\rho^2} & 4q & -\frac{q^2}{p^2} - \frac{p}{\rho} & u + \frac{2q}{p} & 1 \\ 0 & 5k & -\frac{2kq}{p^2} & \frac{2k}{p} & u \end{bmatrix} \begin{bmatrix} \rho \\ u \\ p \\ q \\ k \end{bmatrix}_{,x} = 0. \tag{2.45}$$

A system is hyperbolic if the flux Jacobian, $\underline{f}_{,\underline{q}}$, has only real eigenvalues and a full set of eigenvectors. To examine the hyperbolicty of the closure, we compute the five eigenvalues

of the flux Jacobian:

$$\begin{aligned}
\lambda_1 &= u, \\
\lambda_2 &= u + \frac{q}{2p} - \frac{\sqrt{-3p^4q^2\rho^2 + 4p^5\rho^2\left(k + \frac{p^2}{\rho} + \frac{q^2}{p}\right) - 4\sqrt{\alpha}}}{2p^3\rho}, \\
\lambda_3 &= u + \frac{q}{2p} + \frac{\sqrt{-3p^4q^2\rho^2 + 4p^5\rho^2\left(k + \frac{p^2}{\rho} + \frac{q^2}{p}\right) - 4\sqrt{\alpha}}}{2p^3\rho}, \\
\lambda_4 &= u + \frac{q}{2p} - \frac{\sqrt{-3p^4q^2\rho^2 + 4p^5\rho^2\left(k + \frac{p^2}{\rho} + \frac{q^2}{p}\right) + 4\sqrt{\alpha}}}{2p^3\rho}, \\
\lambda_5 &= u + \frac{q}{2p} + \frac{\sqrt{-3p^4q^2\rho^2 + 4p^5\rho^2\left(k + \frac{p^2}{\rho} + \frac{q^2}{p}\right) + 4\sqrt{\alpha}}}{2p^3\rho},
\end{aligned} \tag{2.46}$$

where

$$\alpha = -p^8\left(-q^2 + p\left(k + \frac{p^2}{\rho} + \frac{q^2}{p}\right)\right)\rho^3\left(p^3 + q^2\rho - p\left(k + \frac{p^2}{\rho} + \frac{q^2}{p}\right)\rho\right). \tag{2.47}$$

We find that each eigenvalue has a distinct eigenvectors

$$\begin{aligned}
r_1 &= \left[1, \lambda_1, \lambda_1^2, \lambda_1^3, \lambda_1^4\right]^T, \\
r_2 &= \left[1, \lambda_1, \lambda_2^2, \lambda_2^3, \lambda_2^4\right]^T, \\
r_3 &= \left[1, \lambda_3, \lambda_3^2, \lambda_3^3, \lambda_3^4\right]^T, \\
r_4 &= \left[1, \lambda_4, \lambda_4^2, \lambda_4^3, \lambda_4^4\right]^T, \\
r_5 &= \left[1, \lambda_5, \lambda_5^2, \lambda_5^3, \lambda_5^4\right]^T.
\end{aligned} \tag{2.48}$$

And we note that one of the waves is linearly degenerate, while the remaining are nonlinear:

$$\begin{aligned}
\nabla_q\lambda_1 \cdot r_1 &\equiv 0, \\
\nabla_q\lambda_2 \cdot r_2 &\not\equiv 0, \\
\nabla_q\lambda_3 \cdot r_3 &\not\equiv 0, \\
\nabla_q\lambda_4 \cdot r_4 &\not\equiv 0, \\
\nabla_q\lambda_5 \cdot r_5 &\not\equiv 0.
\end{aligned} \tag{2.49}$$

A theorem proven by Johnson [8] and Fox et al. [18] gives the condition for hyperbolicity.

Theorem 1 (Johnson 2017 and Fox 2018)**.** *Under the assumptions of the primitive variables*

1. *Positive density:* $\rho > 0$,

2. *Positive pressure:* $p > 0$,

3. *Positive k:* $k > 0$,

then the system is strictly hyperbolic.

Additionally $\{\underline{q} \in \mathbb{R}^5 : \rho(\underline{q}) > 0, p(\underline{q}) > 0, k(\underline{q}) > 0\}$ *is a convex set.*

This hyperbolicity condition is exactly the condition from the Hamburger moment problem for the case $S = 4$ (see Section 2.1).

This concludes our discussion of the moment closure method. Since we now have accomplished closing the problem, we can examine the numerical method used to solve the new system. We discuss the the locally implicit discontinuous Galerkin method in the next chapter.

CHAPTER 3. LOCALLY-IMPLICIT DISCONTINUOUS GALERKIN METHOD

In Chapter 2 we derived and explained the system of partial differential equations (PDEs) to be studied in this work. In this chapter we provide the details of the base numerical method that we developed for solving these PDEs. In particular, we choose to use a locally-implicit Lax-Wendroff discontinuous Galerkin method, in which space is discretized via the discontinuous Galerkin finite element method, and time is discretized via a Lax-Wendroff (aka Cauchy-Kowaleski) expansion.

We consider in this chapter generic one-dimensional conservation laws of the form:

$$\underline{q}_{,t} + \underline{f}\left(\underline{q}\right)_{,x} = \underline{0}, \tag{3.1}$$

where t is time, x is space, $q(t,x) :\in \mathbb{R}^+ \times \mathbb{R} \mapsto \mathbb{R}^{M_{\text{eqn}}}$ is the vector of conserved variables, M_{eqn} is the number of equations, and $\underline{f}\left(\underline{q}\right) : \mathbb{R}^{M_{\text{eqn}}} \mapsto \mathbb{R}^{M_{\text{eqn}}}$ is the flux function. We assume that this system is hyperbolic, meaning that the flux Jacobian:

$$\underline{f}\left(\underline{q}\right)_{,\underline{q}} : \mathbb{R}^{M_{\text{eqn}}} \mapsto \mathbb{R}^{M_{\text{eqn}} \times M_{\text{eqn}}}, \tag{3.2}$$

has real eigenvalues and a complete set of eigenvectors over some convex region $\mathcal{D} \subset \mathbb{R}^{M_{\text{eqn}}}$ in solution space inside of which we are interested in solving the equation.

3.1 Discontinuous Galerkin Method

To discretize equation (3.1) in space we use the discontinuous Galerkin (DG) finite element method, which was first introduced by Reed and Hill [17]. It was fully developed for time-dependent hyperbolic conservation laws in a series of papers by Bernardo Cockburn, Chi-Wang Shu, and collaborators (see [2] and references therein for details).

We define the finite element space

$$\mathcal{W}^h := \left\{ w^h \in [L^\infty(\Omega)]^{M_{\text{eqn}}} : w^h|_{\mathcal{T}_i} \in [\mathbb{P}(M_{\text{deg}})]^{M_{\text{eqn}}} \quad \forall \mathcal{T}_i \right\}, \tag{3.3}$$

where $h = \Delta x = (x_{\text{high}} - x_{\text{low}})/M_{\text{elem}}$ is a uniform gird spacing with M_{elem} being the number of elements. Additionally, M_{eqn} is the number of conserved variables, M_{deg} is the maximal polynomial degree, and the computational mesh is described by non-overlapping elements of width Δx centered at the points x_i:

$$\mathcal{T}_i = \left[x_i - \frac{\Delta x}{2}, x_i + \frac{\Delta x}{2} \right] \qquad \text{for } i = 1, \ldots, M_{\text{elem}}. \tag{3.4}$$

The expression for $\mathcal{W}^h$ basically means that on an element $\mathcal{T}_i$, $\underline{w}$ is a polynomial in $\mathbb{P}(M_{\text{deg}})$ and we do not assume any continuity across elements. On each element we define the local variable, ξ which is related to the spatial variable x by

$$x = x_i + \left(\frac{\Delta x}{2} \right) \xi \qquad \text{for } \xi \in [-1, 1]. \tag{3.5}$$

On each element we approximate the solution by a finite expansion in terms of the following orthonormal Legendre polynomial basis functions:

$$\underline{\Phi} = \left(1, \sqrt{3}\xi, \frac{\sqrt{5}}{2}(3\xi^2 - 1), \frac{\sqrt{7}}{2}(5\xi^3 - 3\xi), \frac{\sqrt{9}}{8}(35\xi^4 - 30\xi^2 + 3), \ldots \right), \tag{3.6}$$

with the orthonormality property:

$$\frac{1}{2} \int_{-1}^{1} \underline{\Phi}\, \underline{\Phi}^T \, d\xi = \mathbb{I}, \tag{3.7}$$

where $\mathbb{I}$ is the identity matrix. On each element we approximate the solution as follows:

$$\underline{q}^h \left(t^n, x_i + \frac{\Delta x}{2} \xi \right) := \underline{\Phi}(\xi)^T \underline{\underline{Q_i^n}}, \tag{3.8}$$

where

$$\underline{\underline{Q_i^n}} \approx \frac{1}{2} \int_{-1}^{1} \underline{\Phi}(\xi) \left[\underline{q} \left(t^n, x_i + \frac{\Delta x}{2} \xi \right) \right]^T \, d\xi \in \mathbb{R}^{M_{\text{O}} \times M_{\text{eqn}}}, \tag{3.9}$$

where $M_{\text{O}} = M_{\text{deg}} + 1$ is the order of accuracy.

3.2 Lax-Wendroff Time Stepping

The Lax-Wendroff method [11] is a fully discrete method for hyperbolic conservation laws. The method is based on the Cauchy-Kovalevskaya [20] procedure to convert time derivatives into spatial derivatives. Starting from a Taylor series in time:

$$\underline{q}\,(t+\Delta t,x)=\underline{q}\,(t,x)+\Delta t\,\underline{q}_{,t}\,(t,x)+\frac{1}{2}\Delta t^2\,\underline{q}_{,t,t}\,(t,x)+\cdots\,, \tag{3.10}$$

we replace all time derivatives using conservation law (3.1) and its derivatives:

$$\underline{q}_{,t}=-\underline{f}(\underline{q})_{,x},\qquad \underline{q}_{,t,t}=-\underline{f}(\underline{q})_{,x,t}=\left[\underline{f}(\underline{q})_{,\underline{q}}\underline{f}(\underline{q})_{,x}\right]_{,x},\qquad \ldots, \tag{3.11}$$

and obtain the following expansion in time:

$$\begin{aligned}\underline{q}(t+\Delta t,x)&=\underline{q}+\Delta t\,\underline{q}_{,t}+\frac{1}{2}\Delta t^2\,\underline{q}_{,t,t}+\ldots &(3.12)\\ &=\underline{q}+\Delta t\,\left[\underline{f}(\underline{q})+\frac{1}{2}\Delta t\,\underline{f}(\underline{q})_{,\underline{q}}\,\underline{f}(\underline{q})_{,x}+\ldots\right]_{,x} &(3.13)\\ &=q+\Delta t\,[F(q)]_{,x}\,, &(3.14)\end{aligned}$$

where the right-hand side is all evaluated at (t,x).

However, the Taylor expansion by hand becomes tedious and messy very quickly. Therefore, we employ the reformulation of Gassner et al. [6] of the Lax-Wendroff discontinuous Galerkin (LxW-DG) scheme [16] in terms of a locally-implicit prediction step, followed by an explicit correction step. This prediction step handles the Taylor expansion for us, so relieving us of the burden of performing the expansion by hand.

3.3 Prediction Step

In the prediction step, we do not enforce consistency with the conservation law, allowing us great freedom. We choose to use primitive variables for this step, which are: $\underline{\alpha}=(\rho,u,p,q,k)$. The prediction step is completely local on each element and therefore, we can focus on the space-element $\mathcal{T}_i$ over time interval $[t^n,t^{n+1}]$, where $t^{n+1}=t^n+\Delta t$. Let

$t = t^n + \frac{\Delta t}{2}(1+\tau)$, for $\tau \in [-1,1]$ and

$$\underline{\alpha}_{,\tau} = \underline{\Theta}(\underline{\alpha}) := -\frac{\Delta t}{\Delta x}\underline{\underline{B}}(\underline{\alpha})\underline{\alpha}_{,\xi}, \tag{3.15}$$

where $\underline{\underline{B}}(\underline{\alpha})$ is the Jacobian matrix. We introduce a Legendre basis on each element,

$$\Psi_\ell(\tau,\xi) = \Phi_{\ell_\tau}(\tau)\Phi_{\ell_\xi}(\xi) \tag{3.16}$$

which is orthonormal on $[-1,1]^2$

$$\frac{1}{4}\int_{-1}^{1}\int_{-1}^{1} \underline{\Psi}\,\underline{\Psi}^T\, d\tau\, d\xi = \underline{\underline{\mathbb{I}}}. \tag{3.17}$$

We write the predicted solution as:

$$\underline{\alpha}^{\mathrm{ST}}\left(t^n + \frac{\Delta t}{2}(1+\tau),\, x_i + \frac{\Delta x}{2}\,\xi\right) := \underline{\Psi}\,(\tau,\xi)^T\,\underline{\underline{W_i^{n+\frac{1}{2}}}}, \qquad \underline{\underline{W_i^{n+\frac{1}{2}}}} \in \mathbb{R}^{M_{\mathrm{P}}\times M_{\mathrm{eqn}}}, \tag{3.18}$$

for $(\tau,\xi) \in [-1,1]^2$, where $\underline{\underline{W}}$ represents the matrix of unknown coefficients, and $M_{\mathrm{P}} = M_{\mathrm{O}}(M_{\mathrm{O}}+1)/2$ are the number of space-time basis functions. Multiplying $\underline{\alpha}_{,\tau} = \underline{\Theta}(\underline{\alpha})$ by the test function $\underline{\Psi}$, we integrate over $(\tau,\xi) \in [-1,1]^2$. We integrate-by-parts in τ and find

$$\begin{aligned}\underline{\underline{L}}\;\underline{W_{i\,(:,m)}^{n+\frac{1}{2}}} = &\frac{1}{4}\int_{-1}^{1}\int_{-1}^{1} \Theta_m\left(\underline{\Psi}^T\underline{\underline{W_i^{n+\frac{1}{2}}}}\right)\underline{\Psi}\, d\tau\, d\xi \\ &+ \left[\frac{1}{4}\int_{-1}^{1} \underline{\Psi}\,(-1,\xi)\;\underline{\Phi}\,(\xi)^T\; d\xi\right]\;\underline{A_{i\,(:,m)}^n},\end{aligned} \tag{3.19}$$

where

$$\underline{\underline{L}} = \frac{1}{4}\int_{-1}^{1}\int_{-1}^{1} \underline{\Psi}\,\underline{\Psi}_{,\tau}^T\, d\tau\, d\xi + \frac{1}{4}\int_{-1}^{1} \underline{\Psi}_{|_{\tau=-1}}\underline{\Psi}_{|_{\tau=-1}}^T\, d\xi, \tag{3.20}$$

$$\underline{\underline{A_i^n}} = \frac{1}{2}\sum_{a=1}^{M_{\mathrm{O}}} \omega_a\,\underline{\Phi}\,(\mu_a)\left[\underline{\alpha}\left(\underline{\Phi}\,(\mu_a)^T\,\underline{\underline{Q_i^n}}\right)\right]^T, \tag{3.21}$$

and $\underline{\alpha}(\underline{q})$ gives the relationship between conservative and primitive variables. Equation (3.19) is a nonlinear algebraic equation that must be solved on each space-time element for the matrix of unknown coefficients: $\underline{\underline{W_i^{n+\frac{1}{2}}}}$.

One common choice for solving a nonlinear equation is to use Newton's method, but this strategy has a couple problematic features. First, Newton's method involves finding

and inverting a Jacobian matrix at every step, which is a costly operation. Second, we must calculate the residual at each iteration and compare it to some tolerance to determine when to end the method, which again increases the number of operations necessesary in each iteration.

An alternative to Newton's method in the current context is to use the simple fixed point scheme known as the Picard iteration. In this method we treat all of the right-hand side of (3.19) as previous iteration information, while only the left-hand side is new iteration information. Practically, this means that we only need to invert one matrix in each iteration: $\underline{\underline{L}}$. Luckily, this matrix is independent of the solution as well as the specific element; and therefore, we can calculate and invert the matrix one time. Additionally, the Picard iteration ends in a small number of iterations, eliminating the need to compute a residual. After replacing all the integrals in (3.19) by Gaussian quadrature rules of the appropriate accuracy, the Picard iteration then gives us

$$\begin{aligned} \underline{W_{i\,(:,m)}^{n+\frac{1}{2}}} \leftarrow & \frac{1}{4}\sum_{a=1}^{M_{\mathrm{O}}}\sum_{b=1}^{M_{\mathrm{O}}} \omega_a\,\omega_b\,\underline{\hat{\Psi}}\,(\mu_b,\,\mu_a)\;\Theta_m\left(\underline{\Psi}\,(\mu_b,\mu_a)^T\,\underline{\underline{W_i^{n+\frac{1}{2}}}}\right) \\ & +\frac{1}{4}\sum_{b=1}^{M_{\mathrm{O}}}\omega_b\,\underline{\hat{\Psi}}\,(-1,\xi_b)\;\underline{\Phi}\,(\xi_b)^T\,\underline{A_{i\,(:,m)}^n}, \end{aligned} \tag{3.22}$$

for $m = 1,\ldots,M_{\mathrm{eqn}}$, where $\underline{\hat{\Psi}} = \underline{\underline{L}}^{-1}\underline{\Psi}$ and ω_a and μ_a for $a = 1,\ldots,M_{\mathrm{O}}$ are the weights and abscissas of the M_{O}-point Gauss-Legendre quadrature rule. This gives a solution for the prediction step, which we know is not consistent with the conservation law, since the step was completely local in space. Therefore, we implement a correction step to regain the correct global nature of the problem.

3.4 Correction Step

The correction step is designed to work like a single forward Euler-like step that uses the predicted solution. To perform this step, we begin with the hyperbolic conservation law (3.1) and multiply by the spatial basis functions defined in (3.6). Next, we integrate over

the space-time element $[t^n, t^n + \Delta t] \times [-1, 1]$:

$$\frac{1}{2\Delta t} \int_{t^n}^{t^n + \Delta t} \int_{\xi=-1}^{\xi=1} \left[\underline{\Phi}(\xi)\, \underline{q}_{,t} + \frac{2}{\Delta x}\, \underline{\Phi}(\xi)\, \underline{f}\left(\underline{q}\right)_{,\xi} \right] d\xi\, dt = \underline{0}. \tag{3.23}$$

Making use of the ansatz

$$\underline{q}^h \left(t^n,\, x_i + \frac{\Delta x}{2}\, \xi \right) := \underline{\Phi}\left(\xi\right)^T \underline{\underline{Q_i^n}}, \quad \text{for} \quad \xi \in [-1, 1] \tag{3.24}$$

and integrating-by-parts in space results in the following expression:

$$\begin{aligned} \underline{\underline{Q_i^{n+1}}} &= \underline{\underline{Q_i^n}} + \frac{\nu}{2} \int_{\tau=-1}^{\tau=1} \int_{\xi=-1}^{\xi=1} \underline{\Phi}_{,\xi}\, \underline{f} \left(\underline{\Psi}^T \underline{\underline{W_i^{n+\frac{1}{2}}}} \right) d\xi\, d\tau \\ &\quad - \nu \left(\underline{\Phi}(1) \left[\underline{\mathcal{F}_{i+\frac{1}{2}}^{n+\frac{1}{2}}} \right]^T - \underline{\Phi}(-1) \left[\underline{\mathcal{F}_{i-\frac{1}{2}}^{n+\frac{1}{2}}} \right]^T \right) \\ &\approx \underline{\underline{Q_i^n}} + \frac{\nu}{2} \sum_{a=1}^{M_\mathrm{O}} \sum_{b=1}^{M_\mathrm{O}} \omega_a\, \omega_b\, \underline{\Phi}_{,\xi}\left(\mu_a\right) \left[\underline{f} \left(\underline{\Psi}\left(\mu_b, \mu_a\right)^T \underline{\underline{W_i^{n+\frac{1}{2}}}} \right) \right]^T \\ &\quad - \nu \left(\underline{\Phi}(1) \left[\underline{\mathcal{F}_{i+\frac{1}{2}}^{n+\frac{1}{2}}} \right]^T - \underline{\Phi}(-1) \left[\underline{\mathcal{F}_{i-\frac{1}{2}}^{n+\frac{1}{2}}} \right]^T \right), \end{aligned} \tag{3.25}$$

where $\nu = \Delta t / \Delta x$. In the expressions after the approximation symbol, $\approx$, we replaced all exact integration by Gauss-Legendre quadrature, where ω_a and μ_a for $a = 1, \ldots, M_\mathrm{O}$ are the weights and abscissas of the M_O-point Gauss-Legendre quadrature rule. The time-integrated numerical fluxes are defined using the predicted solution and the Rusanov [19] time-averaged flux:

$$\underline{\mathcal{F}_{i-\frac{1}{2}}^{n+\frac{1}{2}}} := \frac{1}{2} \sum_{a=1}^{M_\mathrm{O}} \omega_a\, \underline{\mathcal{F}}\left(\mu_a\right), \tag{3.26}$$

where the numerical flux at each temporal quadrature point is given by

$$\underline{\mathcal{F}}\left(\tau\right) := \frac{1}{2} \left(\underline{f}\left(\underline{W_\mathrm{R}}(\tau)\right) + \underline{f}\left(\underline{W_\mathrm{L}}(\tau)\right) \right) - \frac{1}{2} \left|\lambda(\tau)\right| \Big(\underline{q}\left(\underline{W_\mathrm{R}}(\tau)\right) - \underline{q}\left(\underline{W_\mathrm{L}}(\tau)\right) \Big), \tag{3.27}$$

where

$$\underline{W_\mathrm{L}}(\tau) := \underline{\Psi}\left(\tau, 1\right)^T \underline{\underline{W_{i-1}^{n+\frac{1}{2}}}}, \qquad \underline{W_\mathrm{R}}(\tau) := \underline{\Psi}\left(\tau, -1\right)^T \underline{\underline{W_i^{n+\frac{1}{2}}}}, \tag{3.28}$$

and $\left|\lambda(\tau)\right|$ is a local bound on the spectral radius of $\underline{\underline{A}}\left(\underline{q}\right)$ in the neighborhood of interface $x = x_{i-\frac{1}{2}}$ and at time τ.

These steps are all it takes to regain the coupling that was neglected in the prediction step. Therefore, we have a solution which is not only consistent with the conservation law, but is also high order. We do however still have some work to do to ensure that the solution is physical. We must be careful to maintain the positivity of the primititve variables ρ, p, k, as was necessary for the hyperbolicity of the system and for moment realizability. We address the limiters utilized to accomplish this in the next chapter.

CHAPTER 4. POSITIVITY AND NON-OSCILLATORY LIMITERS

In this chapter we describe the limiting strategy for nonlinearly stabilizing the base numerical scheme described in Chapter 3. We aim to achieve positivity of density (ρ), pressure (p), and kurtosis (k), and non-oscillatory behavior in the presence of shocks and rarefactions. All of this is accomplished using limiters at various stages in the algorithm.

4.1 Positivity of Local Lax-Friedrichs

Before considering the high-order method with limiters, it is critical for the theoretical development that first-order schemes when applied to the moment-closure model (2.42) described in Chapter 2, are able to maintain positivity. With the below theorem, we are able to prove precisely such a result: the local Lax-Friedrichs method (aka, the Rusanov method) is positivity-preserving under a suitable time-step restriction. See Theorem 2 below for details.

Theorem 2. *Let $\nu = \frac{\Delta t}{\Delta x}$. Let $\underline{Q_i^n}$ and $\underline{Q_i^{n+1}}$ be the solutions produced by the local Lax-Friedrichs scheme for grid cell i at time levels n and $n+1$, respectively. If $\underline{Q_i^n}$ satisfies $\rho_i^n, p_i^n, k_i^n > 0$ for all i, then $\underline{Q_i^{n+1}}$ satisfies $\rho_i^{n+1}, p_i^{n+1}, k_i^{n+1} > 0$ for all i, under the CFL condition:*

$$\nu \max\left(\lambda_{i+\frac{1}{2}}, \lambda_{i-\frac{1}{2}}\right) < 1, \tag{4.1}$$

where

$$\lambda_{i\pm\frac{1}{2}} = \max\left\{\lambda_{\max}\left(\underline{Q_i^n}\right), \lambda_{\max}\left(\underline{Q_{i\pm1}^n}\right), \lambda_{\max}\left(\frac{1}{2}\left(\underline{Q_i^n} + \underline{Q_{i\pm1}^n}\right)\right)\right\}. \tag{4.2}$$

Proof. Recall that the local Lax-Friedrichs scheme can be written as

$$\underline{Q_i^{n+1}} = \underline{Q_i^n} - \nu\left[\underline{\mathcal{F}_{i+\frac{1}{2}}} - \underline{\mathcal{F}_{i-\frac{1}{2}}}\right], \tag{4.3}$$

where the numerical fluxes are given by

$$\underline{\mathcal{F}_{i\pm\frac{1}{2}}} = \frac{1}{2}\left[\underline{f}(\underline{Q_i^n}) + \underline{f}(\underline{Q_{i\pm1}^n})\right] - \frac{1}{2}\lambda_{i\pm\frac{1}{2}}\left(\underline{Q_i^n} - \underline{Q_{i\pm1}^n}\right). \tag{4.4}$$

Therefore, we have

$$\begin{aligned}\underline{Q_i^{n+1}} &= \underline{Q_i^n} - \frac{\nu}{2}\left[\underline{f}\left(\underline{Q_{i+1}^n}\right) - \underline{f}\left(\underline{Q_{i-1}^n}\right) - \lambda_{i+\frac{1}{2}}\left(\underline{Q_{i+1}^n} - \underline{Q_i^n}\right) + \lambda_{i-\frac{1}{2}}\left(\underline{Q_i^n} - \underline{Q_{i-1}^n}\right)\right] \\ &= \left(1 - \frac{\nu}{2}\left(\lambda_{i+\frac{1}{2}} + \lambda_{i-\frac{1}{2}}\right)\right)\underline{Q_i^n} + \frac{\nu}{2}\lambda_{i+\frac{1}{2}}\left(\underline{Q_{i+1}^n} - \frac{1}{\lambda_{i+\frac{1}{2}}}\underline{f}\left(\underline{Q_{i+1}^n}\right)\right) \\ &+ \frac{\nu}{2}\lambda_{i-\frac{1}{2}}\left(\underline{Q_{i-1}^n} + \frac{1}{\lambda_{i-\frac{1}{2}}}\underline{f}\left(\underline{Q_{i-1}^n}\right)\right).\end{aligned} \tag{4.5}$$

Under the CFL condition, we easily see that

$$1 - \frac{1}{2}\nu\left(\lambda_{i+\frac{1}{2}} + \lambda_{i-\frac{1}{2}}\right) > 0. \tag{4.6}$$

Therefore, in order to address the positivity of each parameter $\rho_i^{n+1}, p_i^{n+1}, k_i^{n+1}$, we need to prove that

$$\rho\left(\underline{Q_{i\pm1}^n} \mp \frac{1}{\lambda_{i\pm\frac{1}{2}}}\underline{f}\left(\underline{Q_{i\pm1}^n}\right)\right) > 0, \tag{4.7}$$

$$p\left(\underline{Q_{i\pm1}^n} \mp \frac{1}{\lambda_{i\pm\frac{1}{2}}}\underline{f}\left(\underline{Q_{i\pm1}^n}\right)\right) > 0, \tag{4.8}$$

$$k\left(\underline{Q_{i\pm1}^n} \mp \frac{1}{\lambda_{i\pm\frac{1}{2}}}\underline{f}\left(\underline{Q_{i\pm1}^n}\right)\right) > 0. \tag{4.9}$$

For simplicity of the notation, we will not write the subscripts for the remainder of the proof.

We begin by showing that the positivity of density is preserved. We see

$$\lambda\rho\left(\underline{Q} \pm \frac{1}{\lambda}\underline{f}(\underline{Q})\right) = \lambda\rho \pm \rho u. \tag{4.10}$$

Dividing by ρ, we have $\lambda + u > 0$ since $\lambda_{i+\frac{1}{2}} \geq |u|$. Therefore, the positivity of ρ is from time step n to $n+1$.

We next show that the pressure remains positive over time. Observe that

$$\lambda^2 \rho p \left(\underline{Q} \pm \frac{1}{\lambda} \underline{f}(\underline{Q}) \right) = -p^2 \pm q\rho\lambda + p\rho\lambda^2 + q\rho u \pm 2p\rho\lambda u + p\rho u^2. \tag{4.11}$$

We note that this is a quadratic polynomial in λ. Examining the coefficient of the λ^2 term, we find $p\rho > 0$. Therefore, the parabola opens upward. The roots of the polynomial are

$$\begin{aligned} \text{root}_1 &= \frac{\mp q\rho - \sqrt{\rho}\sqrt{4p^3 + q^2\rho} \mp 2p\rho u}{2p\rho}, \\ \text{root}_2 &= \frac{\mp q\rho + \sqrt{\rho}\sqrt{4p^3 + q^2\rho} \mp 2p\rho u}{2p\rho}, \end{aligned} \tag{4.12}$$

but under our CFL condition we have $\lambda_{i\pm\frac{1}{2}} > \text{root}_1$ and $\lambda_{i\pm\frac{1}{2}} > \text{root}_2$. Therefore, pressure is positive.

We finally show that $k_i^{n+1} > 0$. Observe that

$$\begin{aligned} \lambda^3 \rho p k \left(\underline{Q} + \frac{1}{\lambda} \underline{f}\left(\underline{Q}\right) \right) = &-p^2 k\lambda - \rho k^2 \lambda \pm q\rho k\lambda^2 + p\rho k\lambda^3 \mp p^2 ku \mp \rho k^2 u + 2q\rho k\lambda u \\ &\pm 3p\rho k\lambda^2 u \pm q\rho k u^2 + 3p\rho k\lambda u^2 \pm p\rho k u^3. \end{aligned} \tag{4.13}$$

We see that this is a cubic polynomial in λ. We again examine the coefficient of the λ^3 term, and see $p\rho k > 0$. The roots of the polynomial are

$$\begin{aligned} \text{root}_1 &= \mp u, \\ \text{root}_2 &= \frac{-q\rho \mp \sqrt{\rho}\sqrt{4p^3 + q^2\rho + 4p\rho k} - 2p\rho u}{2p\rho}, \\ \text{root}_3 &= \frac{-q\rho + \sqrt{\rho}\sqrt{4p^3 + q^2\rho + 4p\rho k} \mp 2p\rho u}{2p\rho}. \end{aligned} \tag{4.14}$$

Again, under our CFL condition, λ is greater than each of these roots and therefore, k is positive.

Therefore, we have shown that $\rho_i^{n+1}, p_i^{n+1}, k_i^{n+1} > 0$ for all i. □

We have shown that under the correct CFL condition, the first order method will maintain positivity in subsequent time steps. However, higher order methods do not guarantee positivity, so we must implement limiters to correct this.

4.2 Limiter I: Positivity in the Prediction Step

We begin the development of this limiter by first choosing the points at which we will impose positivity, called the positivity points. We chose the Gauss-Legendre points augmented with the end points:

$$\mathbb{X}_{M_{\mathrm{O}}} := \Big\{-1, 1\Big\} \cup \Big\{\text{roots of the } M_{\mathrm{O}}^{\text{th}} \text{ degree Legendre polynomial}\Big\}, \tag{4.15}$$

where M_{O} is the desired order of accuracy. Note that $\mathbb{X}_{M_{\mathrm{O}}}$ contains a total of $M_{\mathrm{O}} + 2$ points. This choice is made because for a fixed order of accuracy, M_{O}, all purely spatial quadrature in the numerical scheme, both internally on the element and on the element faces, will only involve points taken from $\mathbb{X}_{M_{\mathrm{O}}}$.

For the prediction step we require the two-dimensional version of (4.15), which is the Cartesian product of $\mathbb{X}_{M_{\mathrm{O}}}$ with itself:

$$\mathbb{X}^2_{M_{\mathrm{O}}} := \mathbb{X}_{M_{\mathrm{O}}} \otimes \mathbb{X}_{M_{\mathrm{O}}}. \tag{4.16}$$

Therefore, $\mathbb{X}^2_{M_{\mathrm{O}}}$ contains a total of $(M_{\mathrm{O}} + 2)^2$ points. Again, the reason for this choice is that all space-time quadrature in the numerical scheme will involve only points taken from $\mathbb{X}^2_{M_{\mathrm{O}}}$.

In the prediction step, we implement this limiter to ensure the positivity of three of the primitive variables: ρ, p, and k. Following the strategy developed by Zhang and Shu [21] for the Runge-Kutta discontinuous Galerkin scheme, we find the maximum value of $\theta \in [0, 1]$ such that the solution,

$$\begin{aligned} \underline{\alpha}^{\mathrm{ST}}\left(t^n + \frac{\Delta t}{2}(1+\tau),\, x_i + \frac{\Delta x}{2}\,\xi;\, \theta\right) &:= \underline{W^{n+\frac{1}{2}}_{i\,(1,:)}} + \theta \sum_{\ell=2}^{M_{\mathrm{P}}} \Psi_{\,\ell}(\tau,\xi)\, \underline{W^{n+\frac{1}{2}}_{i\,(\ell,:)}}, \\ &= (1-\theta)\, \underline{W^{n+\frac{1}{2}}_{i\,(1,:)}} + \theta\, \underline{\Psi}\,(\tau,\xi)^T\, \underline{\underline{W^{n+\frac{1}{2}}_{i}}}, \end{aligned} \tag{4.17}$$

is positive at the positivity points $\mathbb{X}^2_{M_{\mathrm{O}}}$ for ρ, p, and k. If $\theta = 0$, this means the solution is limited fully, and we are left with the cell average, and $\theta = 1$ implies that no limiting was needed and we are able to use the full high-order approximation. We want to find θ_m, for

$m = 1$ (ρ), $m = 3$ (p), and $m = 5$ (k), such that:

$$(1 - \theta_m)\, W^{n+\frac{1}{2}}_{i\,(1,m)} + \theta_m\, \alpha^m_{\min} = \varepsilon > 0, \quad \alpha^m_{\min} := \min_{(\tau,\xi)\in\mathbb{X}^2_{M_{\mathrm{O}}}} \left\{ \underline{\Psi}\,(\tau,\xi)^T\, \underline{W^{n+\frac{1}{2}}_{i\,(:,m)}} \right\}, \tag{4.18}$$

which is a scalar linear equation that can be easily solved for θ_m:

$$\theta_m = \min \left\{ 1, \frac{W^{n+\frac{1}{2}}_{i\,(1,m)} - \varepsilon}{W^{n+\frac{1}{2}}_{i\,(1,m)} - \alpha^k_{\min}} \right\}. \tag{4.19}$$

This guarantees that going into the correction step, all evaluations will be done beginning with primitive variables that satisfy the correct positivity constraint. Therefore, we only evaluate conserved variables and fluxes inside the convex set $S \in \mathbb{R}^{M_{\mathrm{eqn}}}$ over which the conservation law is hyperbolic. In a practical sense, we avoid computing square roots of negative numbers or dividing by zero. However, this limiting in the prediction step is not sufficient to ensure that in the next step, Q^{n+1}, the solution satisfies the positivity constraint. We also need to apply positivity-preserving limiters in the correction step.

4.3 Limiter II: Positivity of the Cell Average in the Correction Step

In the correction step, we first enforce that the cell average values of ρ, p, and k are positive. This limiting occurs before the numerical update, and here we find a blend of a high order scheme with the Lax-Friedrichs scheme. This limiter closely follows that developed by Moe, Rossmanith, and Seal [14]. As we proved in Theorem 2, the local Lax-Friedrichs scheme is guaranteed to preserve positivity. We compare the cell average of the high order scheme with that of the local Lax-Friedrichs scheme and if the high order method violates positivity, we limit those fluxes to satisfy the positivity conditions.

We begin by computing the high-order numerical fluxes according to the correction flux update:

$$\underline{\mathcal{F}^{n+\frac{1}{2}}_{i-\frac{1}{2}}} := \frac{1}{2} \sum_{a=1}^{M_{\mathrm{O}}} \omega_a\, \underline{\mathcal{F}}\,(\mu_a)\,, \tag{4.20}$$

where the numerical flux at each quadrature point is given by

$$\underline{\mathcal{F}}(\tau) := \frac{1}{2}\left(\underline{f}\left(\underline{W_{\mathrm{R}}}(\tau)\right) + \underline{f}\left(\underline{W_{\mathrm{L}}}(\tau)\right)\right) - \frac{1}{2}|\lambda(\tau)|\Big(\underline{q}\left(\underline{W_{\mathrm{R}}}(\tau)\right) - \underline{q}\left(\underline{W_{\mathrm{L}}}(\tau)\right)\Big), \tag{4.21}$$

where

$$\underline{W_{\mathrm{L}}}(\tau) := \underline{\Psi}(\tau, 1)^T \underline{\underline{W_{i-1}^{n+\frac{1}{2}}}}, \qquad \underline{W_{\mathrm{R}}}(\tau) := \underline{\Psi}(\tau, -1)^T \underline{\underline{W_{i}^{n+\frac{1}{2}}}}. \tag{4.22}$$

We also compute the local Lax-Friedrichs update from $t = t^n$ to $t = t^n + \Delta t$, where we use cell averages $\underline{Q^n_{i(1,:)}}$ as the initial data, giving

$$\underline{Q_i^{LxF}} := \underline{Q^n_{i(1,:)}} - \nu\left(\underline{\mathcal{F}^{\mathrm{LxF}}_{i+\frac{1}{2}}} - \underline{\mathcal{F}^{\mathrm{LxF}}_{i-\frac{1}{2}}}\right), \tag{4.23}$$

where $\nu = \frac{\Delta t}{\Delta x}$. The numerical flux is

$$\underline{\mathcal{F}^{\mathrm{LxF}}_{i-\frac{1}{2}}} := \frac{1}{2}\left[\underline{f}(\underline{Q^n_{i(1,:)}}) + \underline{f}(\underline{Q^n_{i-1(1,:)}})\right] - \frac{1}{2}|\lambda_{i-\frac{1}{2}}|\left(\underline{Q^n_{i(1,:)}} - \underline{Q^n_{i-1(1,:)}}\right), \tag{4.24}$$

where $|\lambda|$ is a local bound on the spectral radius of the flux Jacobian, $\underline{\underline{A}}\left(\underline{q}\right)$, in the neighborhood of interface $x = x_{i-\frac{1}{2}}$ at time $t = t^n$. Recall that Q_i^{LxF} is guaranteed to follow the positivity constraints under a reasonable time-step restriction (see Theorem 2).

We then complete the update of the cell averages using a limited flux:

$$\underline{Q^{n+1}_{i\,(1,:)}} = \underline{Q^{\mathrm{LxF}}_{i\,(1,:)}} - \nu\left(\theta_{i+\frac{1}{2}}\,\underline{\Delta\mathcal{F}_{i+\frac{1}{2}}} - \theta_{i-\frac{1}{2}}\,\underline{\Delta\mathcal{F}_{i-\frac{1}{2}}}\right), \tag{4.25}$$

where

$$\underline{\Delta\mathcal{F}_{i-\frac{1}{2}}} := \underline{\mathcal{F}^{n+\frac{1}{2}}_{i-\frac{1}{2}}} - \underline{\mathcal{F}^{\mathrm{LxF}}_{i-\frac{1}{2}}}. \tag{4.26}$$

We choose the maximum $\theta \in [0, 1]$ such that the updated solution satisfies the positivity constraints. $\theta = 0$ implies that the solution is fully limited down to the positive local Lax-Friedrichs cell average. On the other hand, $\theta = 1$ means that no limiting was necessary and the full high-order flux is used.

Step 1: To find the θ values for the limiter, we begin by setting the initial θ to 1, and we examine the $\Delta\mathcal{F}_{i-\frac{1}{2}(1)}$ and $\Delta\mathcal{F}_{i+\frac{1}{2}(1)}$. Define

$$\Gamma := \frac{Q^{\mathrm{LxF}}_{i(1)} - \varepsilon}{\nu}, \tag{4.27}$$

where $\varepsilon = 10^{-13}$ and $\nu = \frac{\Delta t}{\Delta x}$. We also use Λ as a placeholder to help construct θ.

Step 2: Beginning with density, we examine the flux from the left and the right and consider the following cases:

Case 1. If $\Delta\mathcal{F}_{i-\frac{1}{2}(1)} < 0$ and $\Delta\mathcal{F}_{i+\frac{1}{2}(1)} < 0$, then

$$\Lambda_{\text{left}} = \Lambda_{\text{right}} = \min\left\{1, \frac{\Gamma}{\left|\Delta\mathcal{F}_{i-\frac{1}{2}(1)}\right| + \left|\Delta\mathcal{F}_{i+\frac{1}{2}(1)}\right|}\right\}. \tag{4.28}$$

Case 2. If $\Delta\mathcal{F}_{i-\frac{1}{2}(1)} < 0$ and $\Delta\mathcal{F}_{i+\frac{1}{2}(1)} > 0$ then

$$\Lambda_{\text{left}} = \min\left\{1, \frac{\Gamma}{\left|\Delta\mathcal{F}_{i-\frac{1}{2}(1)}\right|}\right\}. \tag{4.29}$$

Case 3. If $\Delta\mathcal{F}_{i+\frac{1}{2}(1)} < 0$ and $\Delta\mathcal{F}_{i-\frac{1}{2}(1)} > 0$ then

$$\Lambda_{\text{right}} = \min\left\{1, \frac{\Gamma}{\left|\Delta\mathcal{F}_{i+\frac{1}{2}(1)}\right|}\right\}. \tag{4.30}$$

This procedure ensures the positivity of density. We now continue with pressure.

Step 3: We now continue with pressure. We can convert $\underline{Q_i^{\text{LxF}}}$ to pressure via the formula

$$p^{\text{LxF}} = Q_{i(3)}^{\text{LxF}} - \frac{\left(Q_{i(2)}^{\text{LxF}}\right)^2}{Q_{i(1)}^{\text{LxF}}}. \tag{4.31}$$

Setting $\mu_{11} = 1$, $\mu_{10} = 1$, and $\mu_{01} = 1$ we examine three cases.

Case 1. Let

$$\underline{Q^\star} = \underline{\bar{Q}_i} - \nu\left(\Lambda_{\text{right}}\,\underline{\mathcal{F}_{i+\frac{1}{2}}^{n+\frac{1}{2}}} - \Lambda_{\text{left}}\,\underline{\mathcal{F}_{i-\frac{1}{2}}^{n+\frac{1}{2}}}\right), \tag{4.32}$$

and define

$$p^\star = Q_{(3)}^\star - \frac{\left(Q_{(2)}^\star\right)^2}{Q_{(1)}^\star}. \tag{4.33}$$

If $p^\star < 0$, then we set $\mu_{11} = \left(p^{\text{LxF}} - \varepsilon\right)/\left(p^{\text{LxF}} - p^\star\right)$. This concludes the first case, and we continue on to the second case.

Case 2. Let

$$\underline{Q^\star} = \underline{\bar{Q}_i} + \nu \left(\Lambda_{\text{left}} \underline{\mathcal{F}^{n+\frac{1}{2}}_{i-\frac{1}{2}}} \right), \tag{4.34}$$

and reevaluate $p^\star$ (4.33) with this new $\underline{Q^\star}$. If $p^\star < 0$, then $\mu_{10} = \left(p^{\text{LxF}} - \varepsilon\right) / \left(p^{\text{LxF}} - p^\star\right)$. Next, we move to the third and final case.

Case 3. Let

$$\underline{Q^\star} = \underline{\bar{Q}_i} + \nu \left(\Lambda_{\text{right}} \underline{\mathcal{F}^{n+\frac{1}{2}}_{i+\frac{1}{2}}} \right), \tag{4.35}$$

and reevaluate $p^\star$ (4.33) with this new $\underline{Q^\star}$. If $p^\star < 0$, then $\mu_{01} = \left(p^{\text{LxF}} - \varepsilon\right) / \left(p^{\text{LxF}} - p^\star\right)$. Following the conclusion of these three cases, we let $\mu = \min\{\mu_{11}, \mu_{10}, \mu_{01}\}$, and rescale $\Lambda_{\text{left}} = \Lambda_{\text{left}}\mu$ and $\Lambda_{\text{right}} = \Lambda_{\text{right}}\mu$. This update concludes our examination of the pressure, and we move on to examine k.

Step 4: The procedure to limit k is the same as that to limit p, with the only change being a replacement of p^{LxF} and $p^\star$ with k^{LxF} and $k^\star$, respectively, where

$$k^{\text{LxF}} = Q^{\text{LxF}}_{i(5)} - \alpha_1^{\text{LxF}}(\alpha_2^{\text{LxF}})^4 - 6\alpha_3^{\text{LxF}}(\alpha_2^{\text{LxF}})^2 - 4\alpha_4^{\text{LxF}}\alpha_2^{\text{LxF}} - \frac{(\alpha_3^{\text{LxF}})^2}{\alpha_1^{\text{LxF}}} - \frac{(\alpha_4^{\text{LxF}})^2}{\alpha_3^{\text{LxF}}}, \tag{4.36}$$

$$k^\star = Q^\star_{i(5)} - \alpha_1^\star(\alpha_2^\star)^4 - 6\alpha_3^\star(\alpha_2^\star)^2 - 4\alpha_4^\star\alpha_2^\star - \frac{(\alpha_3^\star)^2}{\alpha_1^\star} - \frac{(\alpha_4^\star)^2}{\alpha_3^\star}. \tag{4.37}$$

Here, the primitive variables $\underline{\alpha}^{\text{LxF}}$ and $\underline{\alpha}^\star$ are found by converting from the conservative variables $\underline{Q^{\text{LxF}}}$ and $\underline{Q^\star}$ respectively. We find a new value of μ and rescale Λ_{left} and Λ_{right}.

Recall that at the beginning, we set $\theta = 1$. We now rescale $\theta = \min\{\theta, \Lambda\}$ With this value, we ensure that the cell averages are positive. This concludes the second limiter and we are able to move to the next limiter, which also works in the correction step, but now enforces the positivity condition on the quadrature points.

4.4 Limiter III: Positivity in the Correction Step on the Quadrature Points

Once we have ensured that the cell averages are positive, we then look to enforce positivity at the quadrature points. This looks very similar to the positivity limiter in the prediction step, but this time we are working with the conserved variables. Following the ideas developed by Zhang and Shu [21] for the Runge-Kutta discontinuous Galerkin scheme, the idea is to find the maximum $\theta \in [0,1]$ such that

$$\begin{aligned} \underline{q}^h\left(t^{n+1}, x_i + \frac{\Delta x}{2}\,\xi; \theta\right) &:= \underline{Q^{n+1}_{i\,(1,:)}} + \theta \sum_{\ell=2}^{M_{\mathrm{C}}} \Phi_\ell(\xi)\, \underline{Q^{n+1}_{i\,(\ell,:)}} \\ &= (1-\theta)\, \underline{Q^{n+1}_{i\,(1,:)}} + \theta\, \underline{\Phi}(\xi)^T\, \underline{\underline{Q^{n+1}_i}} \end{aligned} \tag{4.38}$$

satisfies the appropriate positivity constraints at all the quadrature points. Just as before, $\theta = 0$ means that the solution is limited fully down to its cell average, while $\theta = 1$ means that no limiting is needed and the full high-order approximation can be used.

Unlike in the prediction step where are already working in the primitive variables, since we are working in the conserved variables we begin by converting the conserved variables into the three primitive variables that must be positive, ρ, p, and k. We then proceed as we did in the prediction step. We want to find θ_ℓ where $\ell = 1, 3, 5$ such that:

$$(1-\theta_\ell)\, W^{n+\frac{1}{2}}_{i\,(1,\ell)} + \theta_\ell \alpha^\ell_{\min} = \varepsilon > 0, \quad \alpha^\ell_{\min} := \min_{(\tau,\xi)\in\mathbb{X}^2_{M_{\mathrm{O}}}} \left\{ \underline{\Psi}\,(\tau,\xi)^T\, \underline{W^{n+\frac{1}{2}}_{i\,(:,\ell)}} \right\}, \tag{4.39}$$

which is a scalar linear equation that can be easily solved for θ_ℓ:

$$\theta_\ell = \min\left\{ 1, \frac{W^{n+\frac{1}{2}}_{i\,(1,\ell)} - \varepsilon}{W^{n+\frac{1}{2}}_{i\,(1,\ell)} - \alpha^\ell_{\min}} \right\}. \tag{4.40}$$

These new values are then used for the corrected solution. Using these three limiters, we are able to ensure that the positivity conditions, $\rho > 0$, $p > 0$, $k > 0$, are satisfied in our solution.

4.5 Limiter IV: Oscillation Limiter

The previously described limiters guarantee positivity for ρ, p, and k, but there still may be unphysical oscillations at shocks and rarefactions. To eliminate these oscillations, we augment the method with one more limiter. We have found that applying a limiting strategy similar to the one developed by Krivodonova [10]. This limiter is applied once per time step, which is enough to provide sufficient limiting without diffusing the numerical solution. The limiter is applied on the conserved variables. We choose a value $\alpha = 0.5\Delta x^{1.5}$.

The limiter is completed in five steps where we will be looping over grid cells (i). We begin by finding the maximum ($\underline{M}_i$) and minimum ($\underline{m}_i$) where each element of the vector comes from the maximum of each parameter in $\underline{\alpha}$. We also take note of the average value of each cell ($\underline{Q^n_{i(1,j)}}$). Next find

$$\underline{M}_i^\star = \max\{\underline{Q^n_{i(1,j)}} + \alpha, \underline{M}_{i-1}, \underline{M}_{i+1}\}, \tag{4.41}$$

$$\underline{m}_i^\star = \min\{\underline{Q^n_{i(1,j)}} - \alpha, \underline{m}_{i-1}, \underline{m}_{i+1}\}. \tag{4.42}$$

In step three, we begin determining the θ that we will use to control the oscillations using the values computed in the previous steps. Find

$$\underline{\theta}^{\text{tmp}}_{\underline{M}_i} = \min\left\{\frac{\underline{M}_i^\star - \underline{Q^n_{i(1,j)}}}{1.1(\underline{M}_i - \underline{Q^n_{i(1,j)}} + \epsilon)}, 1\right\}, \tag{4.43}$$

$$\underline{\theta}^{\text{tmp}}_{\underline{m}_i} = \min\left\{\frac{\underline{Q^n_{i(1,j)}} - \underline{m}_i^\star}{1.1(\underline{Q^n_{i(1,j)}} - \underline{m}_i + \epsilon)}, 1\right\}. \tag{4.44}$$

With these temporary θ values, we find the minimum over the equations:

$$\theta_{M_i} = \min\{\underline{\theta}^{\text{tmp}}_{\underline{M}_i}\}, \tag{4.45}$$

$$\theta_{m_i} = \min\{\underline{\theta}^{\text{tmp}}_{\underline{m}_i}\}. \tag{4.46}$$

Therefore,

$$\theta_i = \max\{0, \min\{1, \theta_{m_i}, \theta_{M_i}\}. \tag{4.47}$$

Finally, the limiter is applied to the conserved variables:

$$\underline{Q_i^{n+1}} = \theta_i \underline{Q_i^{n+1}}. \tag{4.48}$$

This scaling damps the unphysical oscillations around discontinuities but does not turn on in areas where the solution is smooth.

With these four limiters, we are able to preserve the positivity condition, $\rho > 0$, $p > 0$, and $k > 0$ as well as damp out unphysical oscillations near shocks and rarefactions. These ensure that we have a physical solution and that the hyperbolicity of the system is maintained. We now present the results of a few tests that were run using the locally-implicit Lax-Wendroff DG scheme with the implemented limiters.

CHAPTER 5. NUMERICAL RESULTS

In this section we solve three different shock tube problems with different right and left states. For each problem we plot the primitive variables. All tests were run with the fourth order method.

5.1 Example 1

The shock tube problem is a classical problem used to validate computational fluid models, and therefore was a natural choice as a first test for our method and limiters. The problem is described by a tube with a thin film or diaphragm separating the tube into two sides where the initial states on each side are different. The evolution of the flow is observed when the diaphragm is instantaneously removed. In Figure 5.1 we show a shock tube problem with the initial states

$$(\rho, u, p, q, k)_\ell = (1.5, -0.5, 1.5, 1.0, 2.33), \tag{5.1}$$

$$(\rho, u, p, q, k)_r = (1.0, -0.5, 1.0, 0.5, 1.75). \tag{5.2}$$

The panels of the figure show the (a) density, (b) pressure, (c) velocity, (d) heat flux, and (e) kurtosis. We can see the waves in the result, which from left to right are, a rarefaction, a shock, a contact wave (which does not show up in panels (b), (c), and (d)), a rarefaction, and a final shock.

5.2 Example 2

In Figure 5.2 we show a second shock tube problem with the initial states

$$(\rho, u, p, q, k)_\ell = (1.0, -0.7, 1.5, 1.5, 1.75), \tag{5.3}$$

$$(\rho, u, p, q, k)_r = (0.5, -0.9, 1.0, 1.0, 1.0). \tag{5.4}$$

The panels of the figure show the (a) density, (b) pressure, (c) velocity, (d) heat flux, and (e) kurtosis. We can see the waves in the result, which from left to right are, a shock, a shock, a contact wave (which does not show up in panels (b), (c), and (d)), a rarefaction, and a final shock.

5.3 Example 3

The vacuum problem is described by pulling the gas in two opposite directions, creating a vacuum in the middle. In Figure 5.3 we see this problem with the initial states

$$(\rho, u, p, q, k)_\ell = (1.0, -2.0, 1.0, 0.0, 3.0), \tag{5.5}$$

$$(\rho, u, p, q, k)_r = (1.0, 2.0, 1.0, 0.0, 3.0). \tag{5.6}$$

The panels of the figure show the (a) density, (b) pressure, (c) velocity, (d) heat flux, and (e) kurtosis. We take note that the density, pressure and kurtosis fall very close to zero, but never become negative.

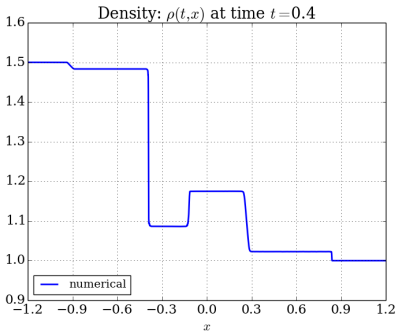

(a)

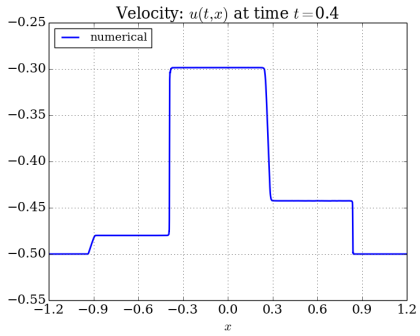

(b)

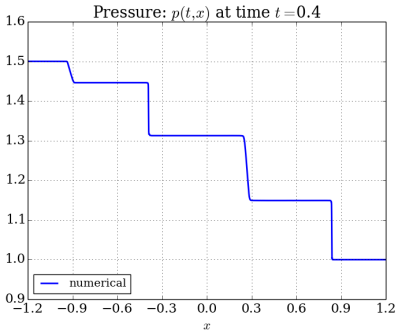

(c)

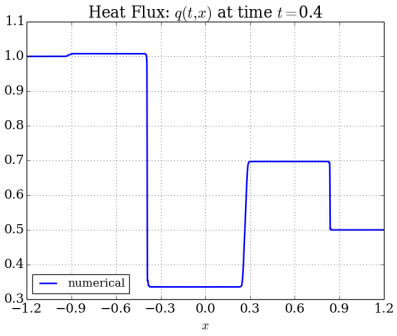

(d)

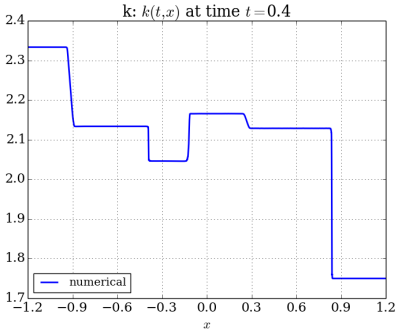

(e)

Figure 5.1: A shock tube problem with initial states $(\rho, u, p, q, k)_\ell = (1.5, -0.5, 1.5, 1.0, 2.33)$ and $(\rho, u, p, q, k)_r = (1.0, -0.5, 1.0, 0.5, 1.75)$. The panels show (a) density, (b) pressure, (c) velocity, (d) heat flux, and (e) kurtosis. We can see the waves in the result, which from left to right are, a rarefaction, a shock, a contact wave (which does not show up in panels (b), (c), and (d)), a rarefaction, and a final shock.

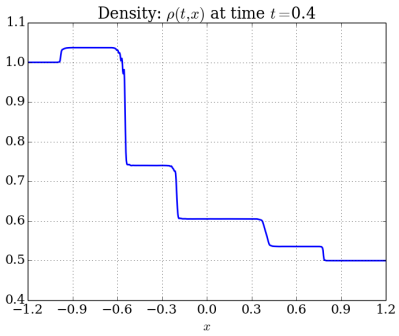

(a)

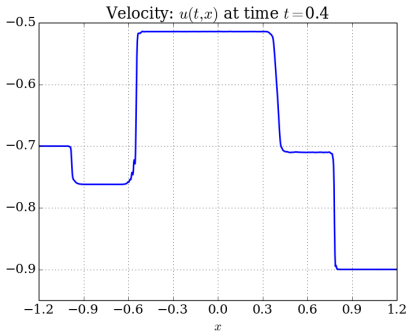

(b)

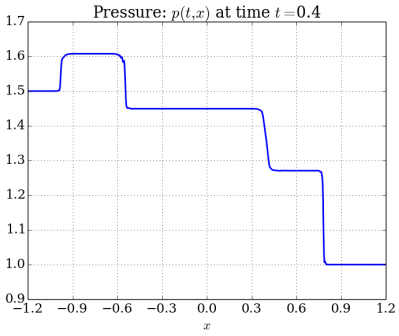

(c)

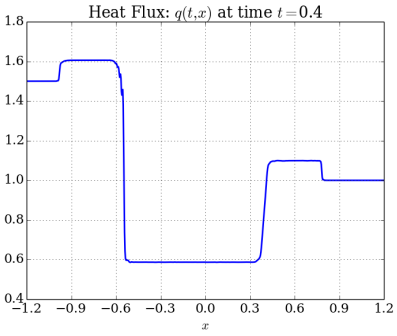

(d)

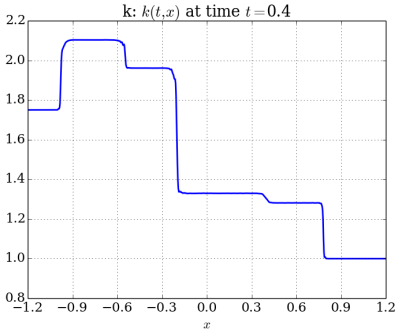

(e)

Figure 5.2: A shock tube problem with initial states $(\rho, u, p, q, k)_\ell = (1.0, -0.7, 1.5, 1.5, 1.75)$ and $(\rho, u, p, q, k)_r = (0.5, -0.9, 1.0, 1.0, 1.0)$. The panels show (a) density, (b) pressure, (c) velocity, (d) heat flux, and (e) kurtosis. We can see the waves in the result, which from left to right are, a shock, a shock, a contact wave (which does not show up in panels (b), (c), and (d)), a rarefaction, and a final shock.

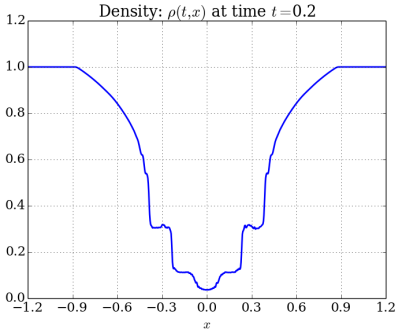

(a)

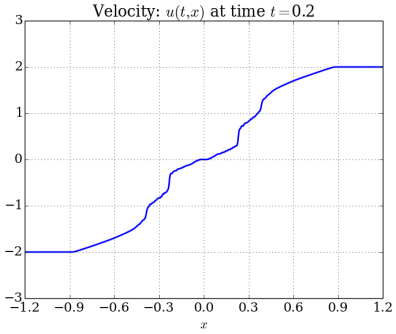

(b)

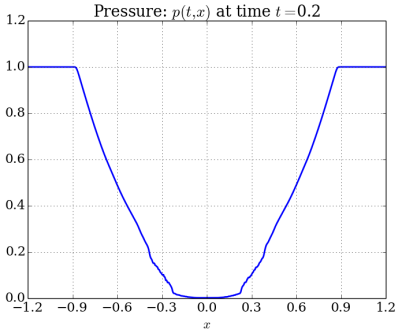

(c)

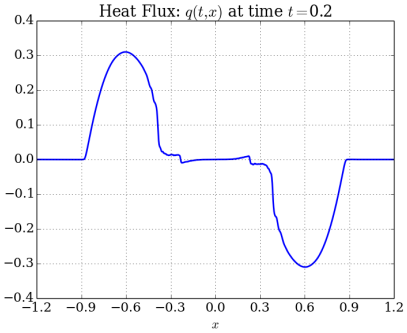

(d)

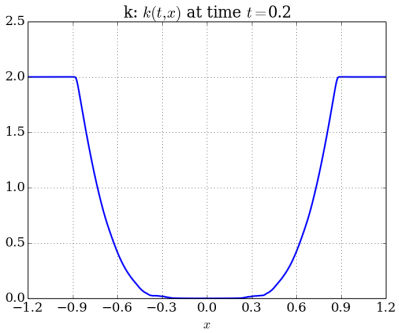

(e)

Figure 5.3: A vacuum problem with initial states $(\rho, u, p, q, k)_\ell = (1.0, -2.0, 1.0, 0.0, 3.0)$ and $(\rho, u, p, q, k)_r = (1.0, 2.0, 1.0, 0.0, 3.0)$. The panels show (a) density, (b) pressure, (c) velocity, (d) heat flux, and (e) kurtosis.

CHAPTER 6. CONCLUSION

6.1 Future Work

Continuing in this project, we hope to explore higher moments and determine accurate ways to close the system. We will draw from the results found by [9] to fit a closure that gives a positive probability function in the acceptable region. This may involve more delta functions or perhaps a different strategy althogether. We also plan to take this into higher dimensions. We will begin by extending the method into two dimensions. A higher dimensional problem poses many challenges, including many more moments and higher computational effort. While there are potential difficulties, it also brings us closer to applying the method to solve problems in multiphase flows.

6.2 Concluding Remarks

In this work we studied the locally implicit Lax-Wendroff discontinuous Galerkin method. We took the resulting system of equations from the hyperbolic quadrature based moment closure method and implemented this numerical method to solve two example one-dimensional problems. We equipped the method with three positivity limiters and one non-oscillatory limiter to ensure that the solution does not have unphysical features. We proved that the Lax-Friedrichs method, which is utilized in the locally implicit Lax-Wendroff DG scheme, preserves positivity under our CFL condition without the use of any limiter. Finally we presented results that show that the limiters are correctly preserving the positivity and reducing oscillations around discontinuities. We plan to extend the method to higher dimensions and study higher moments in the future.

BIBLIOGRAPHY

[1] C.E. Brennen. *Fundamentals of Multiphase Flow*. Cambridge University Press, 2005.

[2] B. Cockburn and C.-W. Shu. The Runge–Kutta discontinuous Galerkin method for conservation laws V. *J. Comput. Physics*, 141(2):199–224, 1998.

[3] W. Dreyer. Maximisation of the entropy in non-equilibrium. *J. Phys. A: Math. Gen*, 20:6505–6517, 1987.

[4] C. Felton, M. Harris, C. Logemann, S. Nelson, I. Pelakh, and J.A. Rossmanith. Pythonic Lax-Wendroff DG code. https://bitbucket.org/imsejae/pythonic_lxw_dg, June 2018.

[5] Rodney O. Fox. Higher-order quadrature-based moment closure methods for kinetic equations. *Journal of Computational Physics*, 228(20):7771–7791, 2009.

[6] G. Gassner, M. Dumbser, F. Hindenlang, and C.-D. Munz. Explicit one-step time discretizations for discontinuous Galerkin and finite volume schemes based on local predictors. *J. Comput. Physics*, 230:4232–4247, 2011.

[7] H. Grad. On the kinetic theory of rarefied gases. *Comm. Pure Appl. Math.*, 2:559–632, 1949.

[8] Erica Renee Johnson. A high-order discontinuous galerkin finite element method for a quadrature-based moment-closure model. Master's thesis, Iowa State University, 2017.

[9] Michael Junk. Maximum entropy for reduced moment problems. *Mathematical Models and Methods in Applied Sciences*, 10(07):1001–1025, 2000.

[10] L. Krivodonova. Limiters for high-order discontinuous Galerkin methods. *J. Comp. Phys.*, 226:879–896, 2007.

[11] P.D. Lax and B. Wendroff. Systems of conservation laws. *Comm. Pure Appl. Math.*, 13:217–237, 1960.

[12] C.D. Levermore. Moment closure hierarchies for kinetic theories. *J. Stat. Phys.*, 83:1021–1065, 1996.

[13] D.L. Marchisio and R.O. Fox, editors. *Multiphase Reacting Flows: Modelling and Simulation*. Springer, 2007.

[14] S. Moe, J.A. Rossmanith, and D.C. Seal. Positivity-preserving discontinuous galerkin methods with lax-wendroff time discretizations. *J. Sci. Comput.*, 71:44–70, 2017.

[15] I. Muller and T. Ruggeri. *Extended Thermodynamics*. Springer, 1993.

[16] J. Qiu, M. Dumbser, and C.-W. Shu. The discontinuous Galerkin method with Lax-Wendroff type time discretizations. *Comput. Methods Appl. Mech. Engr.*, 194:4528—4543, 2005.

[17] W.H. Reed and T.R. Hill. Triangular mesh methods for the neutron transport equation. Technical Report LA-UR-73-479, Los Alamos Scientific Laboratory, 1973.

[18] Aymerc Vie Rodney O. Fox, Frederique Laurent. Conditional hyperbolic quadrature method of moments for kinetic equations. *J. Comp. Phys.*, 2018.

[19] V.V. Rusanov. Calculation of interaction of non-steady shock waves with obstacles. *J. Comp. Math. Phys. USSR*, 1:267–279, 1961.

[20] S. von Kowalesky. Zur Theorie der partiallen Differentialgleichungen. *Journal für die reine und angewandte Mathematik*, 80:1–32, 1875.

[21] X. Zhang and C.-W. Shu. Maximum-principle-satisfying and positivity-preserving high-order schemes for conservation laws: Survey and new developments. *Proc. R. Soc. A*, 467:2752–2776, 2011.